# Design of Electrostatic Actuators for MOEMS Applications

Dooyoung Hah[1,2], Hiroshi Toshiyoshi[1,3], and Ming C. Wu[1]

[1]Department of Electrical Engineering, University of California, Los Angeles
Box 951594, Los Angeles, CA 90095-1594, USA
[2]Microsystem team, Electronics and Telecommunications Research Institute, Korea
[3]Institute of Industrial Science, University of Tokyo, Japan
E-mail: dyhah@etri.re.kr; Tel: +82-42-860-1606; Fax: +82-42-860-6836

## ABSTRACT

We propose a novel method for pull-in analysis in electrostatic actuation. In this method, pull-in angle can be found once the capacitance of electrodes is calculated as a function of rotation angle. This is based on our theory, which is that the pull-in angle only depends on the capacitance but not on spring constants or applied voltage. The theory is derived analytically and its limit of application is described as well. These theory and method can be applied to the translational motion case in the similar fashion. With the proposed method, the computation time can be reduced considerably since it deals with only one domain rather than executing coupled-domain analysis. This method can be used more effectively where the complexity of electrode structures or spring shape is more severe. By way of example, it is applied to the design of three different types of actuators: parallel-plate torsion mirrors, staggered vertical comb-drives, and scanning micromirror with hidden vertical comb-drives. The theoretical results are compared with experimental data as well.

Keywords: electrostatic actuator, pull-in analysis, MOEMS application, parallel-plate type actuator, vertical comb-drive actuator.

## 1. INTRODUCTION

MEMS (Micro-Electro-Mechanical Systems) has become a key enabling technology for optical communication networks. In many applications, electrostatic actuation is desired because of its low power consumption. The power consideration is particularly important for systems with large arrays such as optical crossconnect (OXC). It is well known that electrostatically actuated MEMS devices can exhibit pull-in phenomena. Some applications take advantage of this effect to realize digitally controlled MEMS such as digital micromirror devices [1-2]. Other applications, such as analog beam steering micromirrors, avoid the pull-in effect to extend the stable operation range [3]. Therefore, precise modeling of the pull-in phenomena is important for the design of MOEMS devices. Pull-in can be modeled analytically for simple geometries such as parallel-plate and comb-drive actuators. The actuators used in practical applications often have more complex electrodes, and more sophisticated methods such as coupled-domain finite element analysis are needed to model the effect. This is very time consuming and not suitable for use in the design phase. In this paper, we propose a simple, general formulation for pull-in phenomena in arbitrarily shaped electrodes. This new method is applied to the design of several MOEMS devices. The theoretical results are compared with experimental data, and excellent agreement has been achieved.

## 2. THEORY – PULL-IN PHENOMENA

There are two kinds of torques, the electrostatic torque ($T_e$) and the mechanical restoring torque ($T_r$), involved in the torsional electrostatic actuation. They can be expressed as:

$$T_e(\theta) = \frac{1}{2} V^2 \frac{\partial C}{\partial \theta}, \qquad T_r(\theta) = k\theta, \tag{1}$$

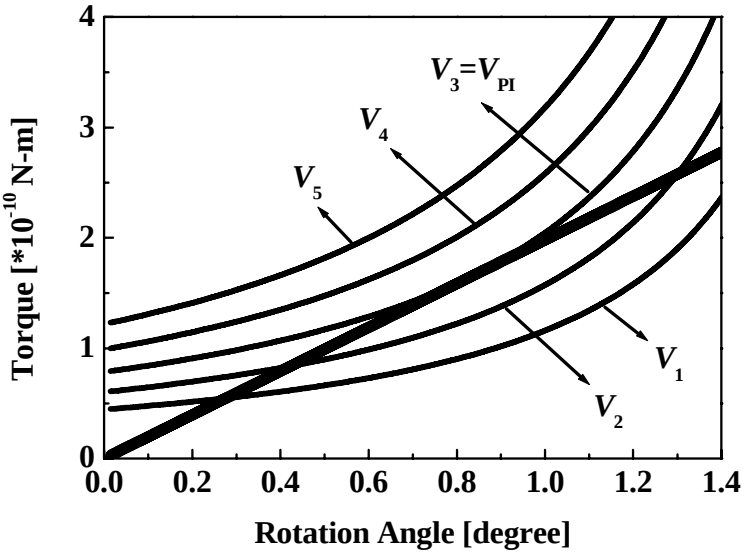


Fig. 1. A typical example of electrostatic torques (thin lines) and mechanical restoring torque (thick line) of an electrostatic actuator.

where $V$, $C$, $\theta$ and $k$ are applied voltage, capacitance of actuator, rotation angle and spring constant, respectively. A typical example curves of these torques is presented in Fig. 1 for various voltages. In the stable region ($V_1$ and $V_2$), both torques are balanced so that the moving electrode stays at certain angle in equilibrium. At the pull-in angle ($\theta_{PI}$ at $V_{PI}$), the electrostatic torque starts overcoming the restoring torque and the moving electrode is abruptly pulled toward the fixed electrode. This, so called, pull-in phenomena happens when both torques are equal and their first derivatives are also equal as plainly shown in Fig. 1. Hence, the pull-in angle satisfies the following two equations.

$$\frac{1}{2}V^2\left(\frac{\partial C}{\partial \theta}\right)_{\theta=\theta_{PI}} = k\theta_{PI} \tag{2a}$$

$$\frac{1}{2}V^2\left(\frac{\partial^2 C}{\partial \theta^2}\right)_{\theta=\theta_{PI}} = k \tag{2b}$$

Combining Eqs. (2a) and (2b) results in one simple equation:

$$\left(\frac{\partial C}{\partial \theta}\right)_{\theta=\theta_{PI}} - \theta_{PI}\left(\frac{\partial^2 C}{\partial \theta^2}\right)_{\theta=\theta_{PI}} = 0\,. \tag{3}$$

The interesting fact is that Eq. (3) is only related to the capacitance, and does not depend on the spring constant or voltage. In other words, the pull-in angle depends only on the geometry of the actuator electrodes. This is valid as long as the actuator satisfies following three conditions: (1) the springs are deformed linearly in the range of consideration, (2) the electrode moves in one dominant direction, i.e., the motion in other directions can be ignored, and (3) the springs and the moving electrode are separated in terms of their roles. From Eq. (3), we can define a general Pull-in Investigation (PI) function,

$$PI(\theta) = \frac{\partial C}{\partial \theta} - \theta \cdot \frac{\partial^2 C}{\partial \theta^2}\,. \tag{4}$$

The solution of equation, $PI(\theta) = 0$, is the pull-in angle. Depending on the actuator structure, there can be multiple solutions for Eq. (3). Multiple solutions means there are several jumps in the transfer (angle-versus-voltage) characteristics. Valid solutions require $\partial C/\partial\theta$ to be positive at that angle. For translational devices, the PI function becomes,

$$PI(x) = \frac{\partial C}{\partial x} - x \cdot \frac{\partial^2 C}{\partial x^2}. \tag{5}$$

These PI functions are very useful to extract pull-in parameters especially when the electrode structure is complicated because it is only related to the capacitance; hence finding solution is much faster than the case of solving two equations (Eq. 2) with torques, voltage, capacitance and angle. After finding the pull-in angle, the pull-in voltage ($V_{PI}$) in the torsion actuator case can be calculated as,

$$V_{PI} = \sqrt{\frac{2k\theta_{PI}}{\left(\partial C/\partial\theta\right)_{\theta=\theta_{PI}}}}. \tag{6}$$

To illustrate the power of this technique, we apply it to the design of three actuators: (1) parallel-plate torsion mirrors, (2) vertical comb actuators, and (3) scanning micromirror with embedded vertical comb drive actuators.

## 3. CASE I – TORSION MIRROR WITH PARALLEL-PLATE ACTUATOR

In parallel-plate torsion mirrors (Fig. 2) [1-3], the capacitance between moving and fixed electrodes ($C_{PP}$) is

$$C_{PP}(\theta) = \frac{\varepsilon_0 W_m}{\theta}\left\{\ln\left(1-\beta\xi\frac{\theta}{\theta_{\max}}\right) - \ln\left(1-\xi\frac{\theta}{\theta_{\max}}\right)\right\}, \tag{7}$$

where $\beta$ is $L_3/L_2$, $\xi$ is $L_2/L_1$ and $\theta_{\max}$ is $H_0/L_1$. In this case, the PI function is

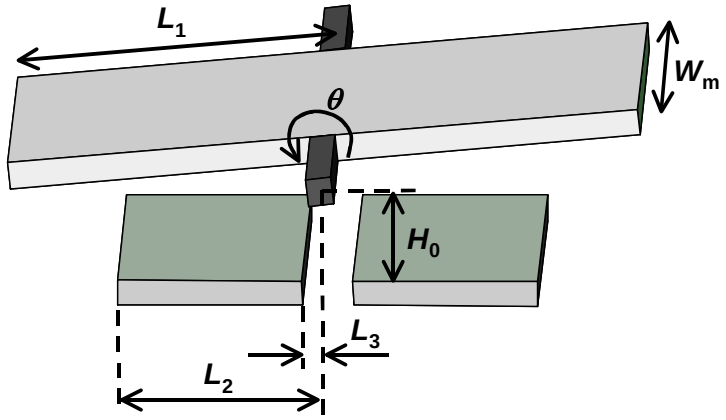


Fig. 2. The schematic diagram of a parallel plate torsion mirror.

$$PI_{PP}(\theta)=\frac{\varepsilon_0 W_e}{\theta^2}\left[\frac{3\dfrac{\xi\theta}{\theta_{\max}}-4\left(\dfrac{\xi\theta}{\theta_{\max}}\right)^2}{\left(1-\dfrac{\xi\theta}{\theta_{\max}}\right)^2}-\frac{3\dfrac{\beta\xi\theta}{\theta_{\max}}-4\left(\dfrac{\beta\xi\theta}{\theta_{\max}}\right)^2}{\left(1-\dfrac{\beta\xi\theta}{\theta_{\max}}\right)^2}+3\ln\left(\frac{1-\dfrac{\xi\theta}{\theta_{\max}}}{1-\dfrac{\beta\xi\theta}{\theta_{\max}}}\right)\right]. \quad (8)$$

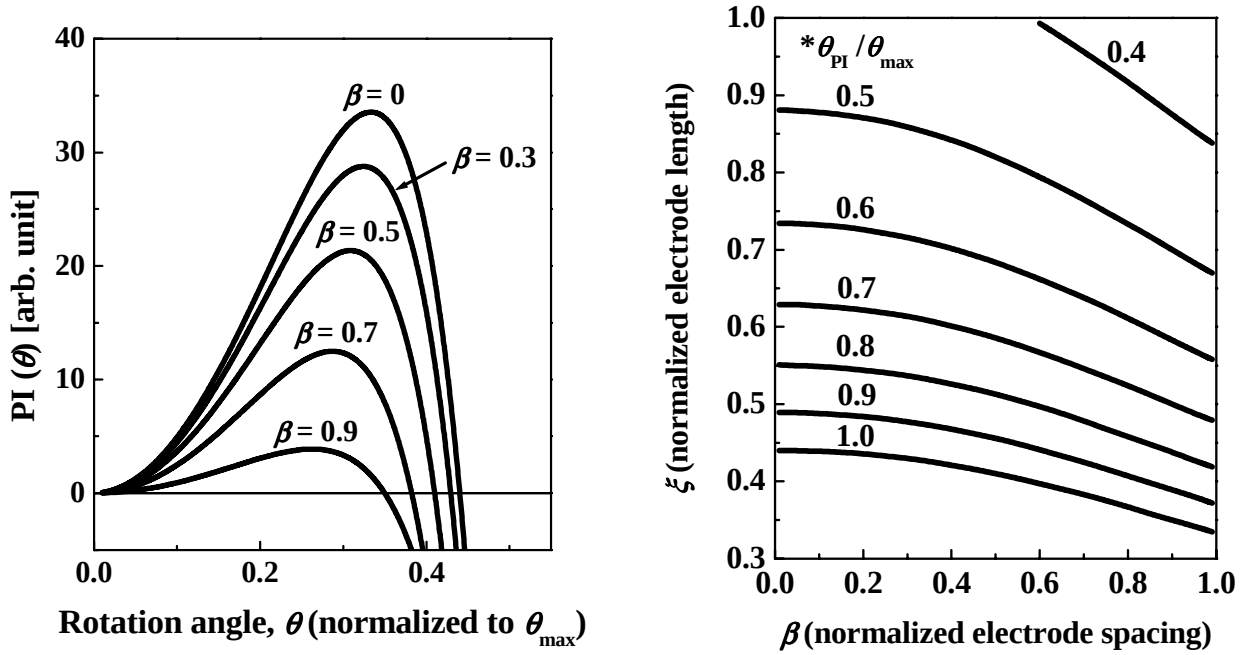


(a) (b)

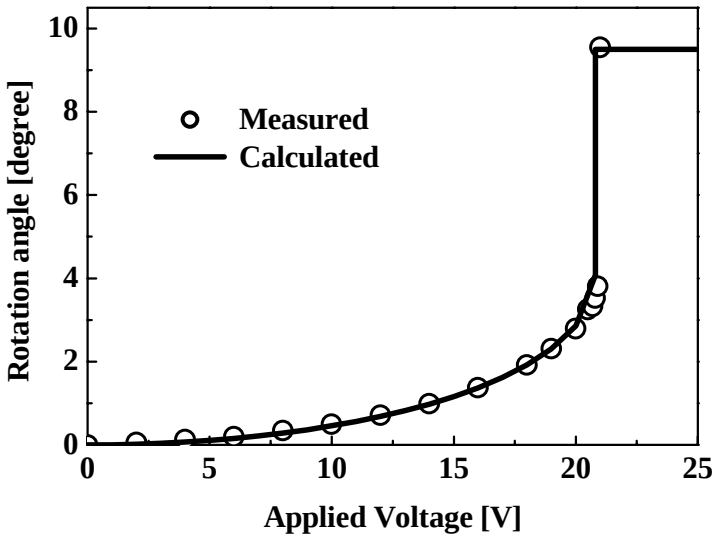


(c)

Fig. 3. (a) The PI function, (b) the electrode geometry contour for the same pull-in angle, and (c) the measured (circle) and the calculated (line) voltage-versus-angle characteristics of the parallel-plate torsion mirror.

Fig. 3(a) shows the PI function of the parallel-plate actuator for various $\beta$ values when $\xi = 1$. The pull-in angle for each $\beta$ can be found at its zero crossing: $PI(\theta) = 0$. The geometries of electrode, $\beta$ (normalized electrode spacing) and $\xi$ (normalized electrode length) values, for the same pull-in angle ($\theta_{PI}$) are drawn in Fig. 3(b). To increase the pull-in angle, both electrode spacing and length should be decreased. When the pull-in angle is equal to $\theta_{max}$, there is no pull-in phenomenon. Fig. 3(c) shows the measured and calculated voltage-vs.-angle characteristic of the parallel-plate torsion actuator. The torsion mirror was fabricated using Sandia National Lab's SUMMiT-V process. The mirror has an area of 135 ($W_m$) × 120 ($2L_1$) μm$^2$. The initial gap between two electrodes ($H_0$) is 10 μm, $\beta$ is 0.53, and $\xi$ is 0.95. The calculated pull-in angle and pull-in voltage are 4.08º and 20.8 V, respectively. These agree very well with the measured values of 3.81º and 20.9 V, respectively.

## 4. CASE II – SCANNING MIRROR WITH STAGGERED VERTICAL COMB DRIVE

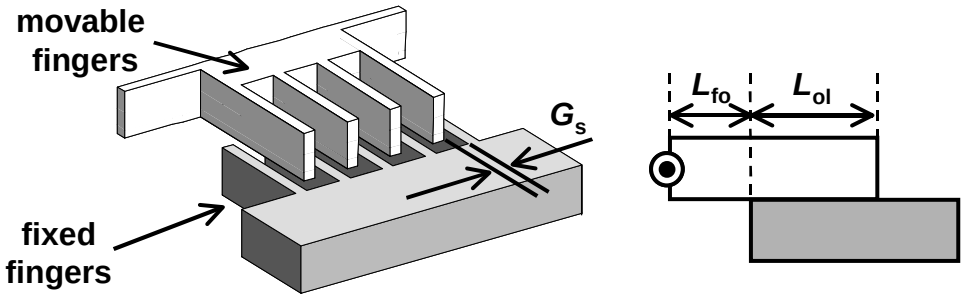


Fig. 4. The staggered vertical comb-drive actuator.

Recently, the staggered vertical comb-drives have been reported as a rotational actuator with the advantages of high electric force density and large continuous rotation angle range [4-5]. In this case (Fig. 4), the capacitance ($C_{SVC}$) can be described as:

$$C_{SVC}(\theta) = \frac{\varepsilon_0 N_f}{G_s}\left(L_{ol} + 2L_{fo}\right)L_{ol}\theta\,, \tag{9}$$

where $N_f$ is the number of fingers. The PI function reduces to a constant:

$$PI_{SVC}(\theta) = \frac{\varepsilon_0 N_f}{G_s}\left(L_{ol} + 2L_{fo}\right)L_{ol} > 0\,. \tag{10}$$

Since this PI function is always positive, the simple staggered vertical comb-drive actuator depicted in Fig. 4 does not have pull-in phenomenon.

## 5. MICROMIRROR WITH HIDDEN VERTICAL COMB DRIVES

The technique we proposed can also be applied to more complex geometries. Fig. 5(a) shows the schematic of a 1-D scanning mirror with hidden vertical comb drive actuators for WDM (wavelength-division multiplexed) Router applications [6]. The actuators and the torsion springs were hidden underneath the mirror to achieve high-fill factor in micromirror arrays. In this case, the fringing capacitance is significant and cannot be ignored. A two-dimensional (2-D) finite element method (FEM) is employed to calculate the capacitance as a function of mirror height. Figure 5(c) shows the electric field distribution in a unit cell. The total capacitance as a function of angle can be calculated by integrating over the finger length. Fig. 6(a) shows calculated PI function for various finger gap spacing ($G_s$). The

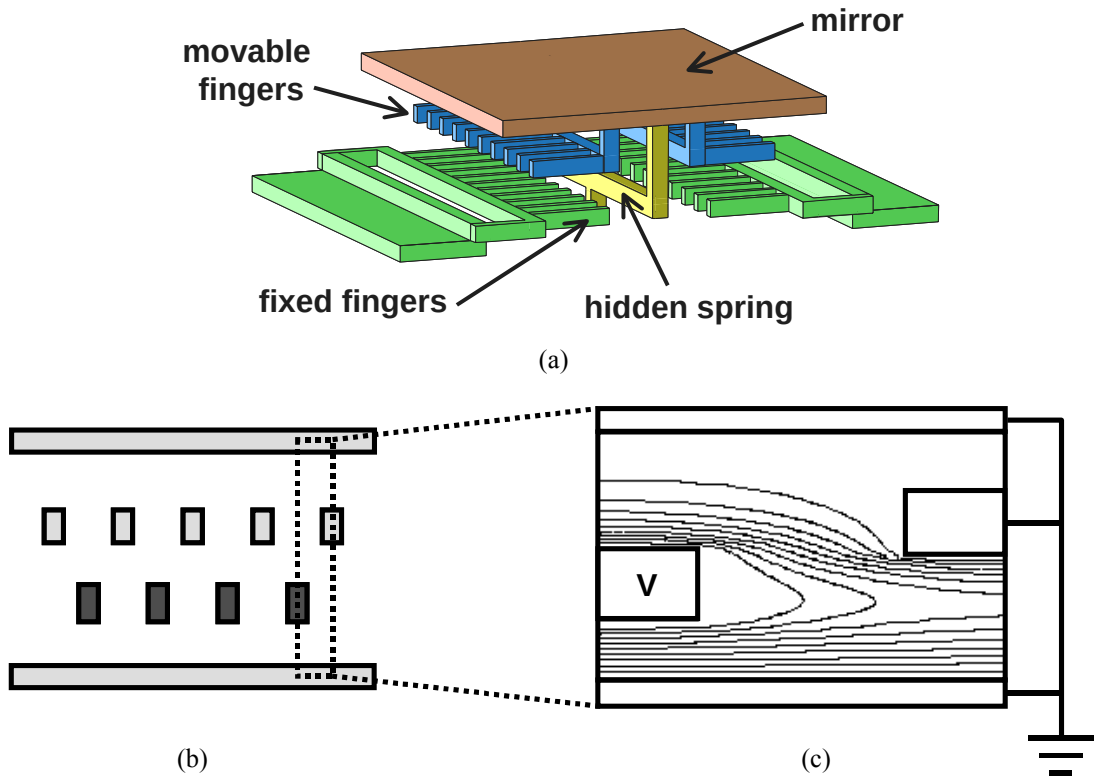


Fig. 5. (a) The schematic diagram and (b) the side-view of the 1-D scanning mirror with hidden vertical comb-drive actuator. (c) Electric field distribution calculated by 2-D finite element method (FEM).

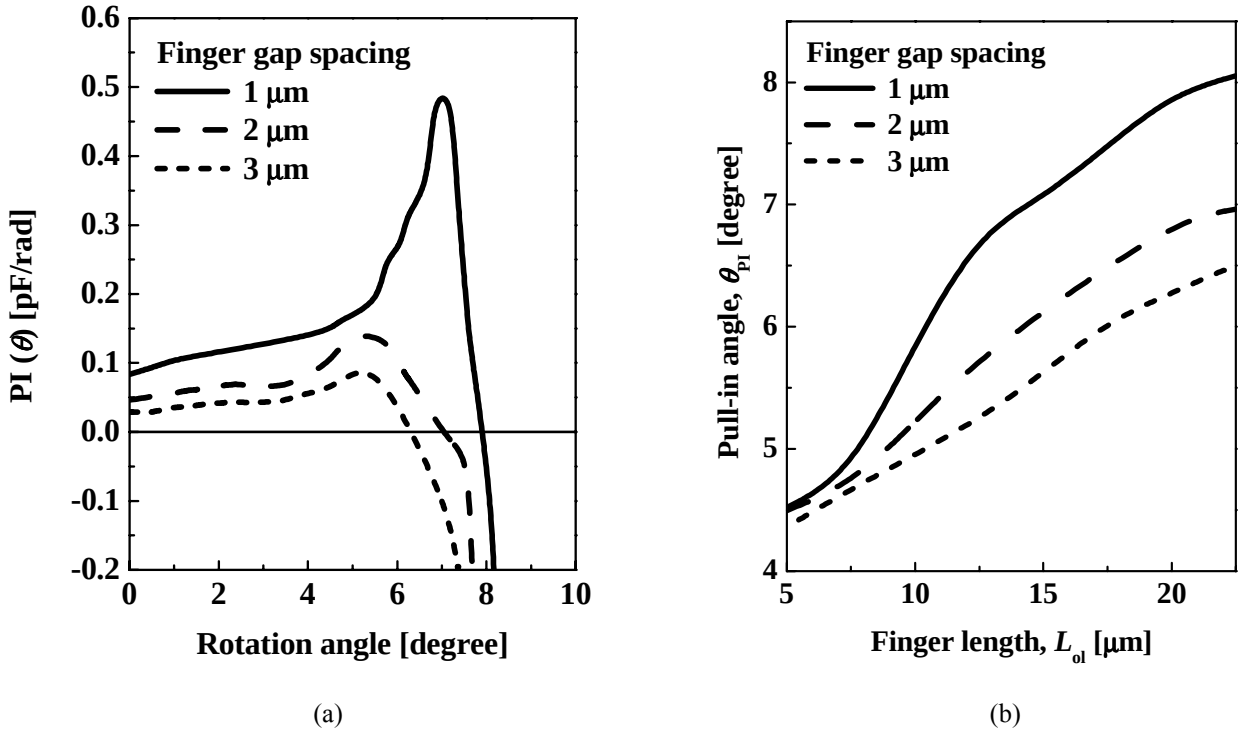


Fig. 6. The calculated (a) PI function and (b) pull-in angle of the 1-D scanning mirror with hidden vertical comb-drive actuator.

calculated pull-in angle is shown in Fig. 6(b). It increases with finger length but decreases with finger spacing. This can be understood by examining various capacitance components. The contributions of comb capacitance become more important when the comb fingers are long and their spacing is narrow. Therefore, the threshold for pull-in increases.

Experimentally, the micromirror array was fabricated by using SUMMiT-V process, taking advantages of its planarization process. The measured and calculated voltage-vs.-angle characteristics of these micromirrors are presented in Fig. 7. The trends of measured and calculated curves agree very well. However, the measured pull-in occurs earlier than the calculated value. The discrepancy may come from the capacitance calculation. We have used a series of 2-D FEM to calculate the capacitance of the 3-D electrodes. More accurate results can be obtained with 3-D FEM.

It should be noted that even with 3-D FEM calculation of capacitance, our method is still much simpler than the full electro-mechanical FDM analysis. The capacitance only needs to be calculated once, and no iterative calculation is needed. Comparing with the conventional analytical approach that solves two equations simultaneously, our method is much more efficient since it deals with only one equation.

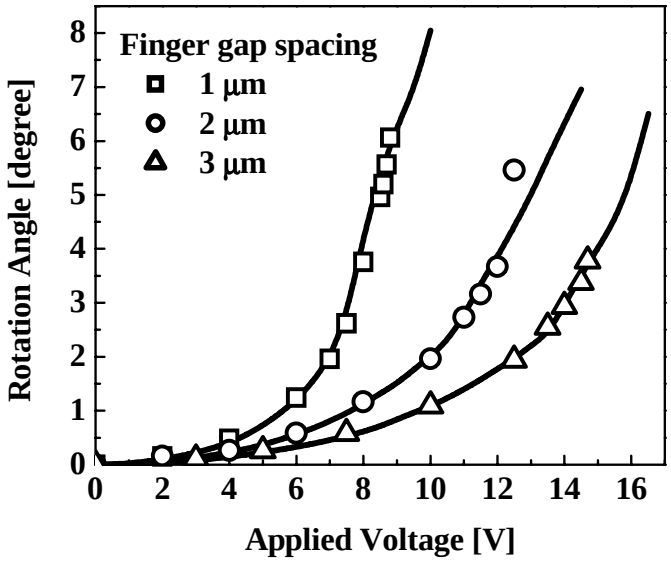


Fig. 7. The measured (symbols) and calculated (lines) voltage-versus-angle characteristics of the 1-D scanning mirror with hidden vertical comb-drive actuators.

## 6. CONCLUSION

In summary, we have proposed a new method to find the pull-in angle (or displacement) of electrostatic actuators. We have shown that the pull-in angle is a function of the capacitance of the actuators only and is independent of the spring constant or voltage. Our method deals with only one equation and is more efficient than the conventional approach. This theory has been applied to the design of three different types of actuators: parallel-plate torsion mirrors, staggered vertical comb-drives, and scanning micromirror with hidden vertical comb-drives. Good agreement with experimental results has been demonstrated.

## 7. ACKNOWLEDGEMENTS

The authors would like to thank Pamela Patterson, Hung Nguyen, Wibool Piyawattanametha and Hsin Chang for technical assistance.

## 8. REFERENCES


[1] P. F. van Kessel, L. J. Hornbeck, R. E. Meier, and M. R. Douglass, "A MEMS-based projection display," Proc. IEEE, vol. 86, no. 8, pp. 1687- 1704, 1998.

[2] J. E. Ford, V. A. Aksyuk, David J. Bishop, and J. A. Walker, "Wavelength add–drop switching using tilting micromirrors," J. Light. Technol., vol. 17, pp. 904-911, 1999.

[3] L. Fan and M. C. Wu, "Two-dimensional optical scanner with large angular rotation realized by self-assembled micro-elevator," Proc. IEEE LEOS Summer Topical Meeting on Optical MEMS, Monterey, Aug. 20–22, 1998, Paper WB4.

[4] J. –L. A. Yeh, H, Jiang, and N. C. Tien, "Integrated polysilicon and DRIE bulk silicon micromachining for an electrostatic torsional actuator," J. Microelectromech. Syst., vol. 8, no. 4, pp. 456-465, 1999.

[5] R. A. Conant, J.T. Nee, K. Lau, and R.S. Muller, "A Flat High-Frequency Scanning Micromirror," 2000 Solid-State Sensor and Actuator Workshop, Hilton Head, SC, pp. 6-9.

[6] D. Hah, S. Huang, H. Nguyen, H. Chang, H. Toshiyoshi, and M. C. Wu, "A low voltage, large scan angle MEMS micromirror array with hidden vertical comb-drive actuators for WDM routers," will be presented in OFC 2002.